Techno-Science Research Journal V14 (Special Issue - EraGET) (2026) P 48-55

Content list available at ITC

Techno-Science Research Journal

Journal Homepage: www.ric.itc.edu.kh

Effect of root orientation and decay on soil shear strength

Roeun Daro[1*], Yoichi Watabe[2]

[1] *Division of Field Engineering for the Environment, Graduate School of Engineering, Faculty of Engineering, Hokkaido University, Sapporo, Hokkaido 060-0813 Japan*

[2] *Division of Civil Engineering, Faculty of Engineering, Hokkaido University, Sapporo, Hokkaido 060-0813 Japan*

Received: 03 November 2025; Revised: 30 July 2026; Accepted: 25 August 2026; Available online: 31 October 2026

Abstract: *Root-reinforced soil is treated as composite material, with mechanical root-soil interactions enhancing soil strength upon shearing; however, its reinforcing effect decreases over time due to plant senescence and root decay. Soil density, influenced by compaction that arranges particles and reduces pore space, determines the soil's ability to support root networks and root-soil interaction. The effect of root network and root decay on shearing behavior relating to difference in soil density remains unclear. In this study, vetiver roots were used to conduct two series of undrained triaxial tests with root decay periods of 45 and 90 days to investigate the shear behavior of root-reinforced soil. The vetiver root volume fixed with 0.74% of total volume of specimen. Two different root networks have been installed with vertical root and vertical-horizontal root segments following compaction density of 1.23 Mg/m^3 and 1.46 Mg/m^3. The compaction density of 1.23 Mg/m^3 has been used to investigate the effects of root orientation and network by installing vertical root and vertical-horizontal root segments with the same volume. Moreover, compaction density of 1.23 Mg/m^3 and 1.46 Mg/m^3 have been prepared for proving the ability of root-soil interaction on the different soil density by installing the same condition of roots orientation (vertical-horizontal) and volume. Finally, the shear behaviors with different root conditions were compared. Vertical root segments had higher at peak shear strength, but lower shear strength at 15% axial strain compared to vertical-horizontal root segments. Moreover, roots in loose soil resist against shearing better than those in dense soil.*

Keywords: Root-reinforced soil, Root decay, Shear strength

1. INTRODUCTION

Root-reinforced soil is a natural-based solution to improve soil strength which is an environmentally friendly approach for controlling soil stabilization and soil erosion [1]. Chrysopogon zizazioides is a vetiver grass widely recognized as an effective and eco-friendly solution to prevent slope failure and surface erosion through root-reinforcement, providing land cover and trapping soil particle on riverbank surfaces [2]. Fibrous roots grow and form a composite material permeating the soil matrix form a soil-root composite structure, demonstrating greater shear strength compared with fallow soil that resists the mobilize loading of soil-root interfacial friction and root tensile properties [3]. In addition, vetiver grass may die due to plant mortality under natural and artificial disturbances such as flooding and agricultural activities (e.g. cutting, burning, applying herbicide) [4]. That could affect a loss of root reinforcement and root-soil interaction as a result of root decomposition, which affects the soil's mechanical and hydraulic properties [5]. The differences in soil density reflect how soil particles are arranged and structured due to compaction or consolidation, depending on the soil deposited conditions. This compaction directly influences root growth, penetration depth, resistance capacity, and network development, as well as ensuring root-soil contact [6]. However, root properties are complicated such as root morphology, orientation, diameters, and strength can vary widely.

The root reinforced mechanism should be explained by identifying the stress paths relevant to slope failure at each position as shown in **Fig. 1**. To protect slope failure, vetiver grass should be planted at the slope crest, surface, and toe. These

* *Correspondence: daro.roeun.o7@elms.hokudai.ac.jp*

DOI : https://doi.org/10.64702/Techno-SRJ.2026.V14.SI2.08
Published by Institute of Technology of Cambodia.
© 2026 INSTITUTE OF TECHNOLOGY OF CAMBODIA. All rights reserved.
This article is an open access article under CC BY-NC-ND 4.0 license.

positions correspond to different stress path of major and minor principle stress of soil elements: the crest and toe are primarily subjected to normal compression and extension, respectively, while the stress states between these positions could follow a direct shear stress path [2]. Moreover, the direct shear tests have been conducted to investigate the changes in soil shear strength due to root reinforcement [4], [7]. However, triaxial testing of root-soil composites has been rarely reported, and several studies have investigated shearing behavior under triaxial compression and extension [2], [8], [9], [10], [11], [12]. Indeed, Karimzadeh et al. [2] studied the effect of root reinforcement under triaxial compression and extension by installing vertical vetiver roots within soil specimen. The results showed that the reinforcing effect was significantly greater under the extension path compared to compression path, where the major principal stress is perpendicular to root orientation. However, only a few studies have examined the influence of root decomposition on the shear strength of root-reinforced soils, particularly for grass or vetiver grass, based on direct shear tests [4], [13]. Kamchoom et al. [13] found a notable change in root decay due to burning required 12 months after vetiver death to cause a 30% shear strength loss, while herbicide caused the same loss in only 2 months. Recently, stress path associated with shearing behavior of decayed roots under triaxial testing has not yet been reported.

The objective of this study is to investigate the shear strength of root-reinforced soil due to root network, root decay, and soil densities under saturated conditions. Two series of undrained triaxial tests, as shown in **Table 1**, were conducted following decay periods of 45 and 90 days compared with reference root-reinforced (assuming no decay) and bare soil specimens. Two different soil compactions were prepared for both bare soil and root-reinforced soil, with dry densities of 1.23 Mg/m^3 and 1.46 Mg/m^3. Series A was conducted with the same compaction soil density of 1.23 Mg/m^3. It consisted of strain-controlled undrained triaxial tests designed to investigate the effects of root reinforcement under different root orientations (vertical and vertical-horizontal root segments) when subjected to triaxial compression at different effective confining stress of 50 and 100 kPa. Series B was prepared with the same root condition (vertical-horizontal root segments) but used two different compaction densities (1.23 Mg/m^3 and 1.46 Mg/m^3) to evaluate the influence of soil density on root-soil interaction behavior under the same triaxial test condition as the first series.

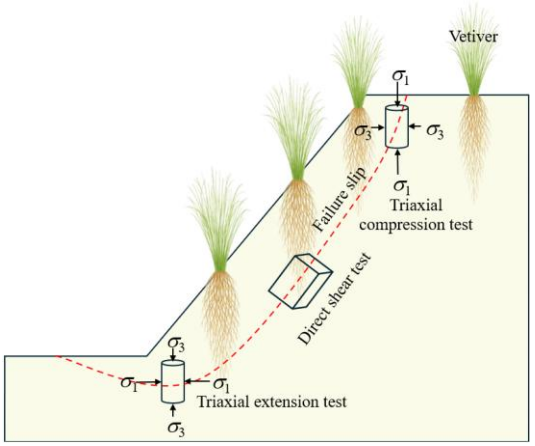


Fig. 1. Rotation of major and minor principal stresses along a failure slip surface with respect to the root orientation.

2. METHODOLOGY

2.1 Material and properties

In this study, reconstituted soil was used for conducting tests. The soil mixture consisted of silica sand (particle size No. 7 and 8) and Kasaoka clay, prepared to achieve target soil properties characteristics of alluvial deposited of Mekong River at the sampled site. The physical properties and particle size distribution curve of the reconstituted soil are demonstrated in **Table 1** and **Fig. 2**.

Vetiver grass is found in many parts of Southeast Asia countries and can grow up to 1 m – 2 m in length after 12 months of growth [14]. Many researchers are interested in using vetiver for shallow slope stabilization. Wu et al. [15] conducted uniaxial tensile test to measure the tensile elastic modulus (161.6 ± 8.98 MPa), tensile strength at breakage (21.4 ± 1.03 MPa) and tensile strain at breakage (0.32 ± 0.01 mm/mm). Phan et al. [4] studied the root decomposition using herbicide, focusing on the effects of root decay on mechanical properties such as tensile strength, secant modulus, breakage strain, and root diameter. The root reinforcement of vetiver retained about 75% of its original value after 112 days of decay. In this study, the mature vetiver grass roots approximately one year old were selected for testing. These roots were brough from Okinawa Green Network NPO Corporation, Okinawa Prefecture, Japan.

Table 1. Triaxial test series and basic soil properties

Triaxial test	ρ_d (Mg/m^3)	Root orientation
Series A	1.23	Vertical
	1.23	Vertical-horizontal
Series B	1.23	Vertical-horizontal
	1.46	Vertical-horizontal
Physical properties		
Specific gravity	G_s = 2.61	

Grain size fraction	Clay = 17%, silt = 25%, fine sand = 58%
Atterberg's limits	LL = 23.5%, PL = 13.52%, PI = 9.98%
USCS soil type	SC
Standard Proctor	w_{opt} = 14%, ρ_{dmax} = 1.82 Mg/m^3

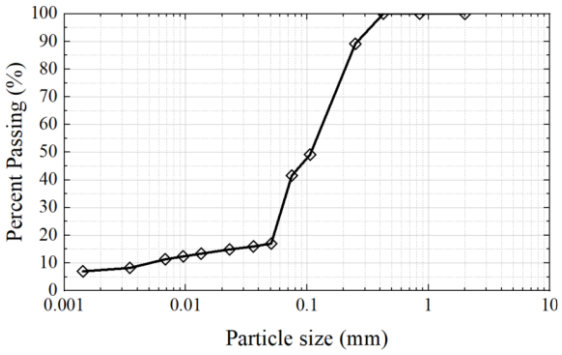


Fig. 2. Particle size distribution.

2.2 Sample preparation

Triaxial test specimens were prepared with identical dimensions, with a height being twice the diameter (70 mm in diameter and 140 mm in height). Two types of specimens were prepared: bare soil (without root) and root-reinforced soil. The bare soil specimens were compacted to achieve target dry densities of 1.23 Mg/m^3 and 1.46 Mg/m^3, corresponding to 67.5% and 80.2% of maximum dry density. Vetiver roots were socked and cleaned in the water, then air-dried for approximately 1 hours before use. A root volume of 4 cm^3 was installed in all root-reinforced specimens, corresponding to a root volume ratio (RVR) of 0.74% of the total specimen volume (538.8 cm^3). The vetiver roots had diameters ranging from 0.48 to 2.29 mm (average 1.46 ± 0.31 mm), and approximately 143 mm for vertical root segments and 70 mm for horizontal root segments. Specimens were prepared by compacting the soil layer by layer while installing roots segments, carefully controlling both mass and volume of specimen. Both the bare soil and root-reinforced specimens were compacted in the same manner, as illustrated in **Fig. 3(b)**. For root-reinforced specimen, the root segments were positioned vertically by pulling them through holes in a circle plastic plate (1.5 mm in diameter and length), as shown in **Fig. 3(a)**. The soil was then compacted to a height of 140 mm at a dry density of 1.23 Mg/m^3 for the series A, which included nine vertical root segments (**Fig. 3(c)** and **Fig. 4(a)**). In the series B, the soil was compacted with five vertical root segments up to a height of 4.7 cm, followed by the installation of four horizontal roots segments for each layer (**Fig. 3(d)** and **Fig. 4(b)**). The process was continued with subsequent root layers as shown in **Fig. 4(b)** for dry density 1.23 and 1.46 Mg/m^3.

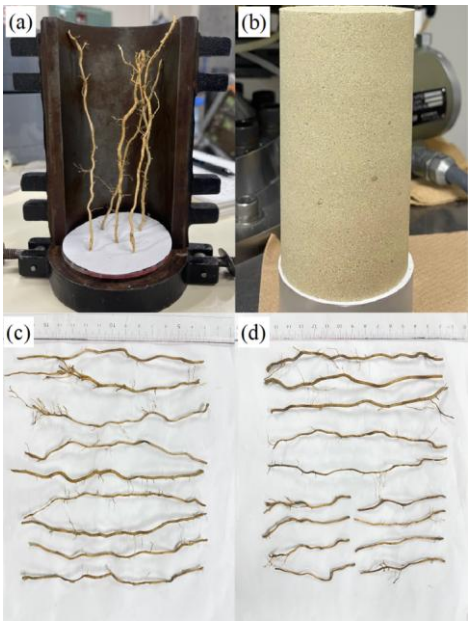


Fig. 3. Root-reinforced specimens' preparation: (a) standing root for soil compaction and (b) compacted specimen, (c) vertical root segments (V root), and (d) vertical-horizontal root segments (VH root).

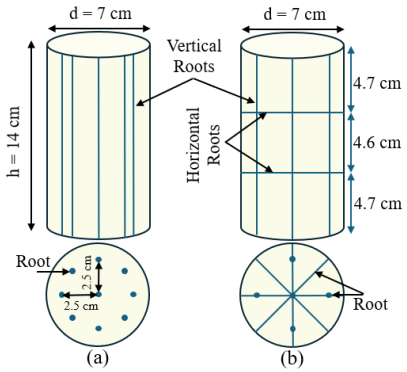


Fig. 4. Geometry of root orientation: (a) V root and (b) VH root.

2.3 Test method and procedures

In this study, isotropic consolidated undrained triaxial compression test was conducted to study the effect of root decay on root-reinforced soil through the two series of tests. Three decay periods of root-reinforced soil specimens were prepared. The first (reference specimens) were tested immediately after the root segments were cut and arranged simultaneously with soil compaction, assuming no decay had occurred. Second and third were tested after periods of 45 and 90 days of root decay, respectively. The 90-day decay period applied in this study based on the flooding period along the Mekong River, where vetiver was fully submerged and died under water, as reported in a previous project, Cambodia – Mekong River Bank Stabilization. The samples preparation described in **Section 2.2**.

The test programmed consisted of two series of root-reinforced and bare soil specimens, which were subjected to

strain-controlled triaxial compression tests at an axial strain rate of 0.1%/min under two different effective pressures (p' = 50 and 100 kPa). The double vacuum method was used, applying negative pressure to remove air from the specimens and allowing water to infiltrate for saturation over approximately one and a half days. Subsequently, back pressure and cell pressure were applied at 300 kPa and 310 kPa to saturate specimens and check degree of saturation based on Skempton's pore pressure parameter. The specimens were considered fully saturated when the B-value exceeded 0.95. After saturation, the specimens were continued to isotropic consolidation under effective confining pressures of 50 and 100 kPa, which were selected based on previous studies [2], [12] and tolerance of testing apparatus. Finally, specimens were sheared to 15% axial strain. Throughout process, roots are considered as fully saturated. **Table 2** summarized the test conditions with experimental parameters.

2.4 Root-soil composites

Typically, a phase diagram in soil mechanics consists of three-phase systems: solids (soil grain), liquids (water in voids), and gases (air in voids). The new model of vegetated soil introduces another phase, roots, which occupy part of the soil pore space. The void ratio of soil containing roots takes into account the presence of this root phase as solid with a specific gravity different from the soil mineral grains [11], [16]. The new formular for soil void ratio, e, for this relationship is following:

$$e = \frac{V_v}{(V_s+V_r)} = \frac{V_{total}-(V_s+V_r)}{(V_s+V_r)} \quad (1)$$

Where V_{total} is total volume of specimen, V_v is volume of voids, V_s is volume of soil grains, and V_r is volume of root.

The root-soil composite provides greater shear resistance than the bare soil specimen due to the ductile behavior of root reinforcement [11]. Moreover, vegetated soil enhances the effective friction angle, cohesion, bonding, and void ratio of the soil [2], [17]. However, the void ratio of soil may increase as roots shrink during decay [18], which also affects to tensile strength of the roots. **Fig. 5** illustrates root morphology and effects of root decay. **Fig. 5(a)** and **(b)** shows the morphology of fresh root planting in laboratory, where the cortex and stele in **Fig. 5(a)** are not fully developed compared to **Fig. 5(b)**, making them susceptible to decay. **Fig. 5(c)** and **(d)** present roots after 90 days of decay under moist and dry conditions, respectively. **Fig. 5(c)** remains in relatively good condition, although the cortex layer becomes compressible, whereas **Fig. 5(d)** shows shrinkage due to dehydration. Therefore, a mature roots system and soil moisture content slow down the root decay process.

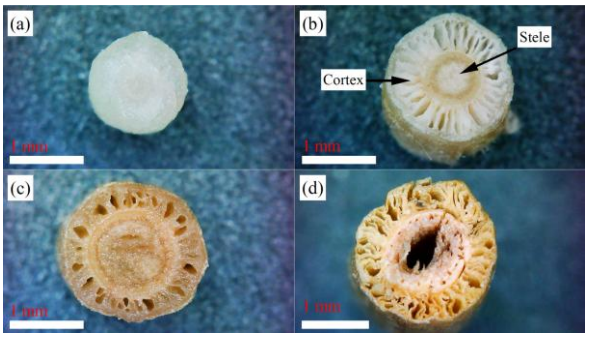


Fig. 5. Root morphology: (a) fresh young root, (b) fresh root, (c) root with 90 days decay, and (d) dry root with 90 days decay.

3. RESULTS AND DISCUSSION

Two series of triaxial tests were conducted to investigate the shear strength of root-reinforced soil at 45 and 90 days of root decay. As described in **Section 2.2**, specimens were prepared with two root orientations (vertical and vertical-horizontal) and two soil densities (1.23 and 1.46 Mg/m^3) for compression tests under effective confining pressure of 50 and 100 kPa. Applying compaction improved the soil particle arrangement, leading to enhanced root-soil interactions. In addition, the saturation and consolidation stages further rearranged the soil particles. During saturation stage, water infiltrated from bottom to top of specimen (simulate as rainfall infiltration). For consolidation, specimen was compression under isotropic conditions, which improved the uniform contact between root and soil.

Table 2. Test conditions and results with the experimental parameters

Decay period	ρ_d (Mg/m^3)	*Root orie.*	p'_c (kPa)	e	M	ϕ'_{cs}	c'
Bare soil	1.23	-	50	1.135	0.81	20.4	0
		-	100	1.134	1.06	25.8	
	1.46	-	50	0.818	1.23	30.3	0.5
		-	100	0.815	1.28	29.3	
No decay	1.23	V	50	1.099	0.82	20.7	0
			100	1.096	1.09	26.5	
	1.23	VH	50	1.098	0.97	24.0	1.1
			100	1.096	1.14	27.5	
	1.46	VH	50	0.778	1.27	30.0	1.2
			100	0.779	1.37	32.0	
45 days decay	1.23	V	50	1.096	0.94	23.3	0
			100	1.097	1.07	26.1	
	1.23	VH	50	1.096	0.94	23.2	0.2
			100	1.098	1.14	27.5	
	1.46	VH	50	0.792	1.35	31.5	0.8
			100	0.793	1.33	31.2	
90 days decay	1.23	V	50	1.097	1.07	26.1	1.9
			100	1.098	1.11	26.8	
	1.23	VH	50	1.099	1.13	27.3	0.6
			100	1.097	1.17	28.1	

1.46	VH	50	0.778	1.31	30.8	0.27
		100	0.789	1.34	31.3	

*Noted**: V= vertical, H = horizontal, orie. = orientation

The specimen after compression test did not depict a clear failure surface at 15% axial strain, including those with higher compaction density. Moreover, the root-soil specimens show more lateral bugling than bare soil and higher shear stress. Roots extracted from specimens were carefully removed and inspected, confirming no root breakage. This indicates that the root reinforcement did not mobilize its full tensile strength during shear. This study, axial strain of 15% remained below the strain required to break the roots diameter of 1–1.5 mm which can withstand up to 30% [15]. Although this strain is sufficient to determine the failure of both the bare and root-reinforced specimens. Foresta et al. [11], using grass species, observed root breakage at the early axial strain (< 10%).

At early axial strain (0.15% and 0.30%) of testing, both bare and root-soil specimen exhibited similar strain-hardening behavior under effective confining stress of 50 and 100 kPa, indicating that root tensile strength has not yet been mobilized. As strain increased, the root-soil composite responded: bare soil reached peak at smaller strain (1.20% and 1.53%) than to root-soil specimens (1.37% to 2.48%), depending on soil density and confining pressure. Vertical root specimen provided higher peak strength but gradually decreased similar to bare soil. Vertical roots were oriented parallel to the major principal stress in compression test. Thus, in this case, the roots bent along the specimen's expansion. In contrast, vertical-horizontal roots were more effective, as they mobilized tensile strength to enhance the soil's shear resistance.

Fig. 6 depicted the stress-strain relationship of root-reinforced and bare soil with two different compaction densities (1.23 and 1.46 Mg/m^3), and two root orientations: V root and VH root. The roots were installed in the specimen for testing at three decay stages: references (assumed no decay), 45 days, and 90 days. **Fig. 6(a)** showed the stress-strain relationship for V root at compaction density of ρ_{d_V} = 1.23 Mg/m^3. The maximum deviator stress (q_{max}) for roots with no decay, 45 days decay, and 90 days decay are 35.6 kPa, 34.8 kPa, 36.1 kPa and 16.6 kPa, 15.9 kPa, 17.9 kPa for effective confining stress of 100 and 50 kPa, respectively. The q_{max} of 45-day decay is slightly lower than no-decay roots, but higher than bare soil, while the q_{max} of 90-day decay is slightly higher than that of no-decay roots. Moreover, axial strain at q_{max} for V root extends to 2.5% and 2.4% before dropping, compared to 1.5% and 1.2% for bare, which reaches q_{max} values of 30.5 kPa and 13.9 kPa for effective confining stress of 100 kPa and 50 kPa, respectively. **Fig. 6(b)** shows the stress-strain relationship of VH root at the same density as in **Fig. 6(a)**. The q_{max} of VH root is slightly lower than V root due to the different number of V root. However, the VH root specimen provides additional tensile resistance against the shearing, causing the deviator stress to decrease more gradually. For the no-decay case at p' = 100 kPa tends to increase deviator stress between 10% and 15% axial strain. At p' = 50 kPa, a similar trend is observed, with the peak maintained until 3.5%, then slightly decreased. For p' = 100 kPa, the deviator stress of 45-day decay roots is lower than no-decay and similar to 90-day decay. At p' = 50 kPa, the deviator stress of 90-day decay is slightly higher than others. **Fig. 6(c)** shows a similar trend to **Fig. 6(b)**, with the same root orientation, but different in soil densities. The deviator stress is substantial at initial axial strain (2.5% and 4.5% for p' = 100 kPa and 50 kPa) and increases until 15% after an initial drop. For p' = 50 kPa, the deviator stress is almost the same for all soil specimens. Notably, root reinforcement contributes more effectively in the lower compaction soil than in higher compaction soil.

Fig. 7 shows stress-path of root-reinforced soil compared with bare soil in different soil densities, root orientations, and influence of root decay the same as **Fig. 6, Fig.7(a)** and **(b)** represent soils with a dry density of 1.23 Mg/m^3 with different root orientation (V root and VH root), while **Fig. 7(c)** represents a denser soil with a dry density of 1.46 Mg/m^3. Each graph shows results for different conditions: bare soil and soil with roots (no-decay, 45-day decay, and 90-day decay), tested under p' = 100 and 50 kPa. The results indicate that the presence of roots significantly enhances soil strength compared with bare soil as discussed in **Fig. 6**, reflected by higher deviator stress on stress-path curve. No-decay root-reinforced soil can represent the upper boundary, and bare soil is lower boundary for the results. For root-reinforced specimen with VH root, a similar behavior was observed, with a slight increase at failure point for p' = 100 kPa, while V root drop. However, under an effective confining stress of p' = 50 kPa, samples show similar trend, and root-reinforced has little effect on compaction soil density of 1.46 Mg/m^3.

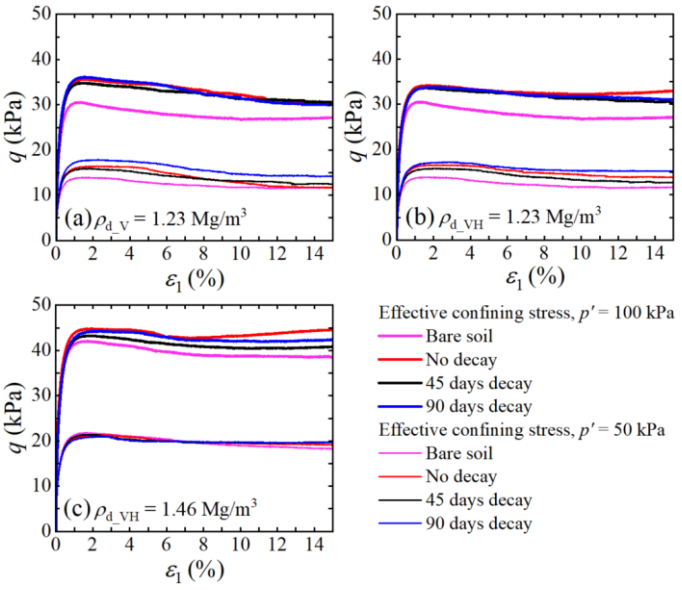


Fig. 6. Stress-strain relationship of root reinforced soil following decay period of 45 days and 90 days: (a) ρ_{d_V} = 1.23 Mg/m^3, (b). ρ_{d_VH} = 1.23 Mg/m^3, and (c). ρ_{d_VH} = 1.46 Mg/m^3.

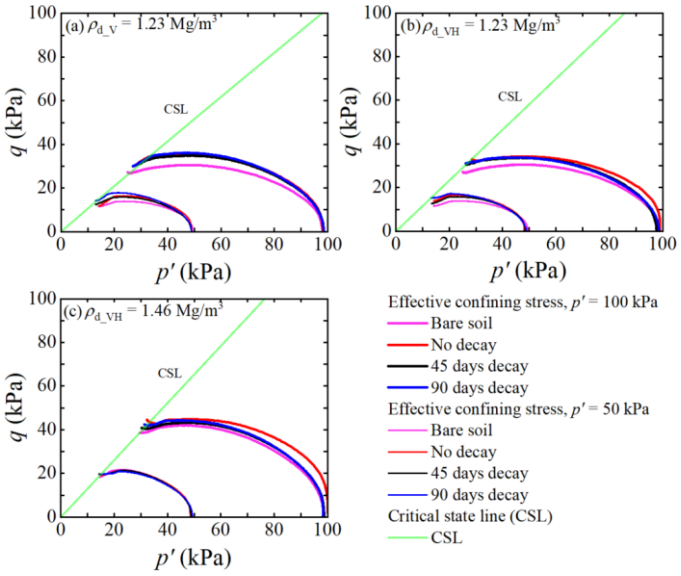


Fig. 7. Stress-path of root reinforced soil following decay period of 45 days and 90 days: (a) ρ_{d_V} = 1.23 Mg/m^3, (b). ρ_{d_VH} = 1.23 Mg/m^3, and (c). ρ_{d_VH} = 1.46 Mg/m^3.

Fig. 8 shows the excess pore water pressure of root-reinforced soil compared with bare soil, for different soil densities and root orientations as same as **Fig. 6**. For p' = 100 kPa, the excess pore water pressure shown a similar trend: the root-reinforced soils show lower excess pore water pressures than the bare soil, but higher than those with no-decay roots, while 45-day and 90-day decay are nearly the same. However, for p' = 50 kPa, the excess pore water pressure are slightly different, with the 90-day decay of the soil density of 1.23 Mg/m^3 is higher values than the others.

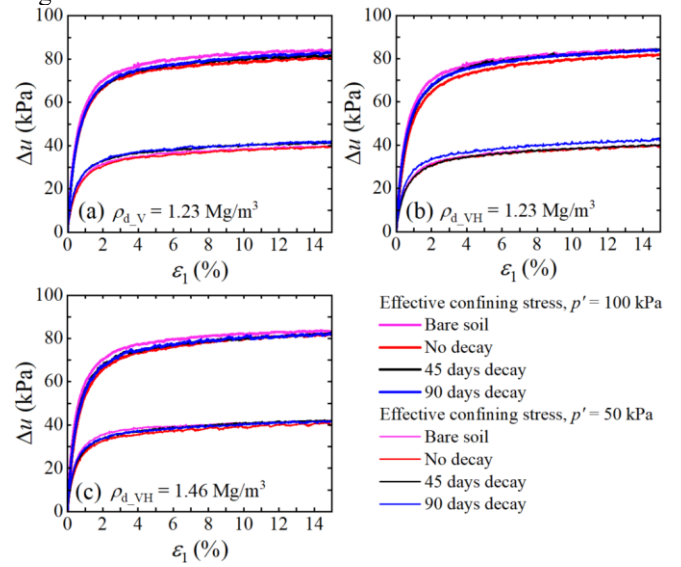


Fig. 8. Excess pore water pressure of root reinforced soil following decay period of 45 days and 90 days: (a) ρ_{d_V} = 1.23 Mg/m^3, (b). ρ_{d_VH} = 1.23 Mg/m^3, and (c). ρ_{d_VH} = 1.46 Mg/m^3.

Fig. 9 presents the comparison of stress-strain relationships according to root orientation, soil compaction density, and normalized deviator stress by the initial mean effective stress, p'_0. **Fig. 9(a)** compares specimens with the same soil density (1.23 Mg/m^3) but different root orientations: V root (black line) and VH root (blue line), under an effective confining stress of p' = 100 kPa. The root-reinforced soil with V root exhibits the highest peak stress ratio (q/p'_0) compared to VH root and bare soil (pink line). However, at 15% axial strain, the VH root specimen shows slightly higher residual stress than V root. **Fig. 9(b)** are the same specimen's condition as **Fig. 9(a)**, but with a difference in effective confining stress (p' = 50 kPa). The overall trend is similar to that in **Fig. 9(a)**, and the root reinforcement supports shear strength to reach the peak stress ratio of q/p'_0 are also comparable. Yet, the peak stress ratio of bare soil under p' = 100 kPa is larger compared to p' = 50 kPa. **Fig. 9(c)** and **(d)** present the results for specimens with the same root orientation but different soil densities and confining effective stress. In **Fig. 9(c)**, under p' = 100 kPa, the specimen with a lower density (1.23 Mg/m^3, blue line) exhibits a larger peak stress ratio for the root-reinforced soil compared with bare soil (pink line) than the specimen with a higher density (1.46 Mg/m^3, red line; pink dotted line for bare soil), while the residual stress is similar. In contrast, **Fig. 9(d)**, under p' = 50 kPa, shows that root reinforcement in the denser soil (1.46 Mg/m^3) provides a slight improvement. However, the root reinforced soil with lower density demonstrates greater strength improvement compared with the bare soil, as observed from both the peak stress ratio and residual stress in **Fig. 9(d)**.

Fig. 10 depicts the critical state friction angle (ϕ'_{cs}) of specimens following decay period. **Fig. 10(a)** and **(b)** presents the critical friction angles of specimens with a soil density of 1.23 Mg/m^3 for bare soil (pink line), V root (black line), and VH

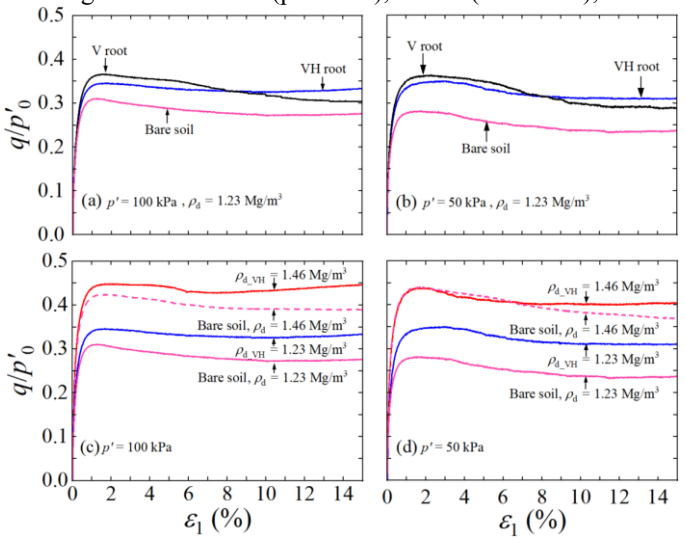


Fig. 9. Comparison of normalized deviator stress and axial strain in different root orientations: (a) and (b), and compaction density: (c) and (d) under effective confining stress of 100 kPa and 50 kPa, respectively.

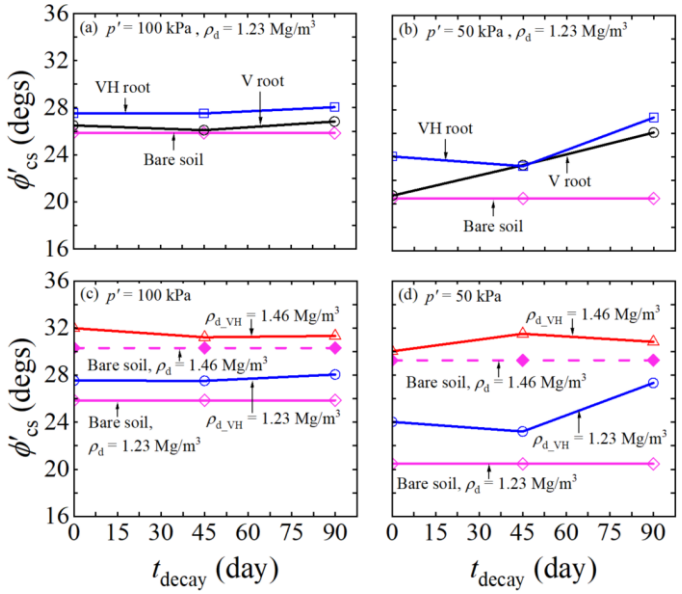


Fig. 10. Comparison of critical friction angle vs decay period roots in different root orientations: (a) and (b), and compaction density: (c) and (d) under effective confining stress of 100 kPa and 50 kPa, respectively.

root (blue line). In **Fig. 10(a)**, where effective confining stress p' = 100 kPa, the critical friction angle of root-reinforced soils was higher than that of bare soil at no-decay, slightly dropped at 45-day decay, and increased at 90-day decay. VH root shows the highest ϕ'_{cs}. **Fig. 10(b)** also shows a greater ϕ'_{cs} for root-reinforced soils. Moreover, at 90-day of decay, the ϕ'_{cs} of the V and VH root specimens under p' = 100 kPa approached similar of **Fig. 10(a)**. **Fig. 10(c)** and **(d)** shows ϕ'_{cs} of VH root specimens with different soil densities (1.23 and 1.46 Mg/m3). For the specimen with a density of 1.46 Mg/m^3 (red line for VH root, pink dotted line for bare soil) under p' = 100 kPa, the friction angle decreased at 45 days of decay and 90 days, which contrasts with specimen under p' = 50 kPa. In general, effective friction angles tend to increase with higher soil density and confining pressure in fine grain soils, which is also evident from the bare soil results. Therefore, root reinforcement had a significant effect on the critical friction angle, particularly by increasing the values at lower confining pressures to levels comparable to those at higher confining pressures. Based on the experimental result, the friction angle would likely reach its maximum when root breakage occurred; however, no root breakage was observed in this experiment. A slight increase in effective cohesion was also observed, as shown in **Table 2**. The effective cohesion of specimens (c') was obtained from Mohr–Coulomb's failure criterion. The equations below were used to determine the slope of the critical state line (M) and the critical friction angle (ϕ'_{cs}):

$$M = \frac{q}{p'} = \frac{6\sin\phi'_{cs}}{3-6\sin\phi'_{cs}} \quad (2)$$

$$\phi'_{cs} = \arcsin\left(\frac{3M}{6+M}\right) \quad (3)$$

Where q = deviator stress, p' = mean effective stress

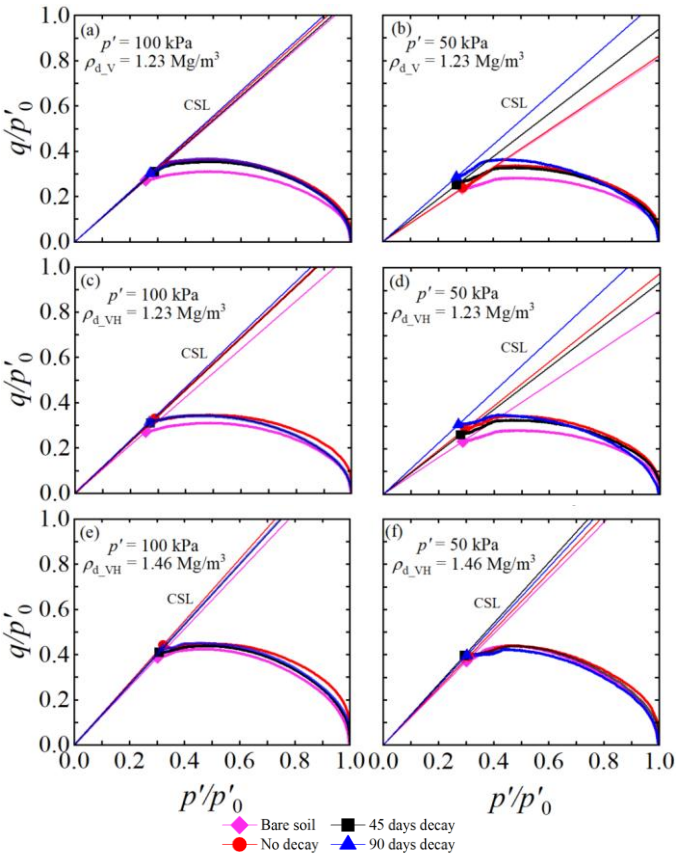


Fig. 11. Stress path normalized by confining under different confining effective stress of 100 kPa and 50 kPa: (a) and (b) ρ_{d_V} = 1.23 Mg/m^3, (c) and (d) ρ_{d_VH} = 1.23 Mg/m^3, and (e) and (f) ρ_{d_VH} = 1.46 Mg/m^3.

Fig. 11 describes the stress paths normalized by the initial mean effective stress under isotropic stress condition to evaluate the effect of root reinforcement under different effective confining stresses and soil densities on slope of critical stage line. The symbols represent bare soil, no-decay, 45-day decay, and 90-day decay conditions, shown by pink diamond, red circle, black square, and blue triangle markers, respectively. The thick curve and thin line of pink, red, black, blue show the stress path (q/p'_0 and p'/p'_0) and slope of critical stage line (M) following decay as markers. **Fig. 11(a)** and **(b)** show V root specimen with soil density of 1.23 Mg/m^3 under p' = 100 and 50 kPa. The M values are approximately 1.1 and below 1.0 (except 90-day decay, 1.07), slightly higher than bare soil. For **Fig. 11(c)** and **(d)** present VH root specimens with the same density and confining stress of **Fig. 11(a)** and **(b)**, showing higher M value than V root cases. **Fig. 11 (e)** and **(f)** are VH root specimen at higher soil density (1.46 Mg/m^3), exhibiting similar behaviour to **Fig. 11(c)** and **(d)**, but with greater M values due to the higher compaction density. Thus, the tensile strength of VH root specimens provided by horizontal roots perpendicular to the direction of the major principal stress (σ'_1) contributed to shear resistance with

increasing axial strain. Consequently, the VH root specimens exhibited higher M values compared to those with V root, as shown in **Table 2**. In addition, the M value of VH root specimens of p' = 50 kPa provided significant reinforcement, reaching a value similar to V root specimen under p' = 100 kPa, consistent with the results observed in critical friction angle.

4. CONCLUSIONS

A comprehensive set of triaxial test results on bare and root-reinforced specimens allows distinguishing the effects of root orientation and soil density of root decay on stress-strain relationship and stress path. The tests were performed under isotropic consolidation and undrained compression with effective confining stresses of p' = 100 kPa and 50 kPa. As a result, the root-reinforced specimen exhibited increasing shear strength compared with bare soil due to the presence of roots. Moreover, the shear strength of the specimens slightly decreased after 45 days of decay and increased after 90 days. This indicates that the three-months decay period, the mature vetiver roots did not have any significant deterioration.

The effect of root orientation was evaluated using specimens with the same soil density and RVR (0.74%). V root specimens showed higher peak deviator stress than VH root, indicating greater resistance to compression at the early stage of axial strain. Beyond this point, the residual stress of VH root is higher than V root at 15% axial strain, indicating that horizontal root segments provided additional shear resistance by acting perpendicular to the major principal stress through horizontal root extension. Vertical root segments bent under shear. Additionally, the contribution of root tensile strength to soil shear resistance was more effectively in soils with lower compaction density and lower effective confining stress.

Soil density and effective confining stress significantly effect on effective stress angle. For bare soil, the dense soil densities and large effective confining stress show a larger critical friction angle than smaller. Meanwhile, the presence of roots caused a noticeable change in critical friction angles. This behavior was slightly different in the root-reinforced specimens.

Future work is being conducted with vetiver-planted soil with well-developed root networks in the laboratory to examine the effects of root reinforcement under different soil compaction densities and root decay periods. The root-reinforced soil will be numerically simulated to evaluate its performance in protecting riverbank slopes under flooding along the Mekong River.

ACKNOWLEDGMENTS

The author would like to acknowledge AUN/SEED-Net of Japan International Cooperation Agency (JICA) for providing graduate scholarship program and Soil Mechanic Laboratory, Faculty of Engineering, Hokkaido University, for supporting this work. The author gratefully acknowledges Okinawa Green Network NPO Corporation, Okinawa Prefecture, Japan, for providing vetiver grass roots and vetiver grass in this research.

REFERENCES

[1] A. Stokes *et al.*, "Ecological mitigation of hillslope instability: ten key issues facing researchers and practitioners," *Plant Soil*, vol. 377, no. 1–2, pp. 1–23, Apr. 2014, doi: 10.1007/s11104-014-2044-6.

[2] A. A. Karimzadeh, A. K. Leung, S. Hosseinpour, Z. Wu, and P. Fardad Amini, "Monotonic and cyclic behaviour of root-reinforced sand," *Can. Geotech. J.*, vol. 58, no. 12, pp. 1915–1927, Dec. 2021, doi: 10.1139/cgj-2020-0626.

[3] G. J. Meijer, D. Muir Wood, J. A. Knappett, A. G. Bengough, and T. Liang, "Root reinforcement: continuum framework for constitutive modelling," *Géotechnique*, vol. 73, no. 7, pp. 600–613, July 2023, doi: 10.1680/jgeot.21.00132.

[4] T. N. Phan, A. K. Leung, V. Kamchoom, and S. Likitlersuang, "Reinforcement losses in soil stabilisation due to decomposing roots of *Chrysopogon zizanioides* and *Chrysopogon nemoralis*," *Land Degrad Dev*, vol. 34, no. 4, pp. 1080–1096, Feb. 2023, doi: 10.1002/ldr.4517.

[5] M. Lei *et al.*, "Temporal evolution of the hydromechanical properties of soil-root systems in a forest fire in China," *Science of The Total Environment*, vol. 809, p. 151165, Feb. 2022, doi: 10.1016/j.scitotenv.2021.151165.

[6] C. Yu *et al.*, "The effects of soil compaction on wheat seedling root growth are specific to soil texture and soil moisture status," *Rhizosphere*, vol. 29, p. 100838, Mar. 2024, doi: 10.1016/j.rhisph.2023.100838.

[7] K. Mahannopkul and A. Jotisankasa, "Influences of root concentration and suction on Chrysopogon zizanioides reinforcement of soil," *Soils and Foundations*, vol. 59, no. 2, pp. 500–516, Apr. 2019, doi: 10.1016/j.sandf.2018.12.014.

[8] D. H. Gray and D. Barker, "Root-soil mechanics and interactions," in *Water Science and Application*, vol. 8, S. J. Bennett and A. Simon, Eds., Washington, D. C.: American Geophysical Union, 2004, pp. 113–123. doi: 10.1029/008WSA09.

[9] H. Rahardjo, A. Satyanaga, E. C. Leong, V. A. Santoso, and Y. S. Ng, "Performance of an instrumented slope covered with shrubs and deep-rooted grass," *Soils and Foundations*, vol. 54, no. 3, pp. 417–425, June 2014, doi: 10.1016/j.sandf.2014.04.010.

[10] M. I. M. Neto and C. F. Mahler, "Study of the Shear Strength of a Tropical Soil with Grass Roots," *S&R*, vol. 40, no. 1, pp. 31–37, Jan. 2017, doi: 10.28927/SR.401031.

[11] V. Foresta, V. Capobianco, and L. Cascini, "Influence of grass roots on shear strength of pyroclastic soils," *Can. Geotech. J.*, vol. 57, no. 9, pp. 1320–1334, Sept. 2020, doi: 10.1139/cgj-2019-0142.

[12] W. He, T. Ishikawa, and B. T. Nguyen, "Effect evaluation of grass roots on mechanical properties of unsaturated coarse-grained soil," *Transportation Geotechnics*, vol. 38, p. 100912, Jan. 2023, doi: 10.1016/j.trgeo.2022.100912.

[13] V. Kamchoom, A. K. Leung, D. Boldrin, T. Sakolpanya, Z. Wu, and S. Likitlersuang, "Shearing behaviour of vegetated soils with growing and decaying roots," *Can. Geotech. J.*, vol. 59, no. 12, pp. 2067–2084, Dec. 2022, doi: 10.1139/cgj-2021-0695.

[14] P. Truong, V. T. Tan, and P. Elise, "The vetiver system for slope stabilization," in *An Engineer's handbook: The Vetiver Network International*, 2008.

[15] Z. Wu, A. K. Leung, D. Boldrin, and S. P. Ganesan, "Variability in root biomechanics of Chrysopogon zizanioides for soil eco-engineering solutions," *Science of The Total Environment*, vol. 776, p. 145943, July 2021, doi: 10.1016/j.scitotenv.2021.145943.

[16] C. W. W. Ng, J. J. Ni, A. K. Leung, and Z. J. Wang, "A new and simple water retention model for root-permeated soils," *Géotechnique Letters*, vol. 6, no. 1, pp. 106–111, Mar. 2016, doi: 10.1680/jgele.15.00187.

[17] C. W. W. Ng, Q. Zhang, S. Zhang, S. Y. Lau, H. Guo, and Z. Li, "A new state-dependent constitutive model for cyclic thermo-mechanical behaviour of unsaturated vegetated soil," *Can. Geotech. J.*, vol. 61, no. 10, pp. 2155–2179, Oct. 2024, doi: 10.1139/cgj-2023-0268.

[18] J. J. Ni, A. K. Leung, and C. W. W. Ng, "Modelling effects of root growth and decay on soil water retention and permeability," *Can. Geotech. J.*, vol. 56, no. 7, pp. 1049–1055, July 2019, doi: 10.1139/cgj-2018-0402.